Description of Thermal Anomalies on Two Active Guatemalan Volcanoes Using Landsat Thematic Mapper Imagery

Robert J. Andres and William I. Rose

Abstract

Santiaguito Dome, Guatemala, continuously extruded dacite lava and underwent daily, vertical, phreatomagmatic eruptions during 1986 to 1988. Three Landsat satellite Thematic Mapper (TM) subscenes recorded this activity over a two-year period. The subscenes show a stationary, high-temperature thermal anomaly around the active vent, Caliente. Two of the subscenes depict vertical ash eruptions, one of which reached 4.5 to 5 km above the dome. The subscenes provide evidence that a recently detected, deep erosional episode on the dome did not begin significantly before February 1988.

At Pacaya Volcano, Guatemala, a basaltic cone in nearly continuous eruption since 1967, a single subscene shows a large, high-temperature thermal anomaly with the characteristics of a basaltic lava flow. Periodic processing of TM images can provide a valuable, supplemental monitoring tool for active volcanoes, particularly when on-site monitoring is limited by economic or personnel resources.

Introduction

A minimum of 158 volcanoes erupted from 1975 to 1985. During this time, approximately 50 more volcanoes showed unrest although eruptions did not occur (McClelland *et al.*, 1989). Limited economic and personnel resources do not allow for close, on-site monitoring of all of these potentially dangerous volcanoes.

This paper further demonstrates the use of commercially available satellite imagery to supplement on-site volcano monitoring by combining several existing techniques and expanding the limits of some of these techniques (Francis and Rothery, 1987; Rothery *et al.*, 1988; Mouginis-Mark *et al.*, 1989; Abrams *et al.*, 1991; Mouginis-Mark *et al.*, 1991; Mouginis-Mark and Francis, 1992). Satellite images are relatively inexpensive, as compared to field campaigns to active volcanoes, and can be analyzed by one person. Also, daily to biweekly coverage can be obtained of an area depending upon the type of satellite used. Four Landsat Thematic Mapper (TM) subscenes of two active Guatemalan volcanoes portray volcanic phenomena not directly observed on the ground by the local monitoring agencies. The morning Landsat orbits precede the buildup of orographic clouds around these volcanoes (Lillesand and Kiefer, 1987).

Background Geology

Santiaguito Dome (14°44'N, 91°34'W, 2520 m) has been erupting dacite since it began to grow in 1922 (Rose, 1972). The magmatic temperature is about 850°C, based on petrography and Fe-Ti oxide data at domes of similar composition (Rose, 1972). The focus of dome extrusion has wandered between several vents over the years. The currently active vent, Caliente, is the site of frequent vertical ash eruptions which give rise to water-rich plumes that contain varying amounts of volcanic ash (Andres, 1992; Andres *et al.*, 1992).

Pacaya (14°22'N, 90°36'W, 2552 m) is an active volcano on the south side of a 100-km^2 caldera (Eggers, 1971; Wunderman and Rose, 1984). It has erupted basalts in a series of eruptions which have created and destroyed a series of composite and cinder cones (Eggers, 1971; Eggers, 1983; Bornhorst *et al.*, 1984; A. MacKenney, personal communication). More complete descriptions of recent activity at these two volcanoes can be found in Andres (1992).

Landsat Images

Landsat satellites provide regular, nearly global coverage and their TM sensor provides 30-m ground resolution in six spectral bands (three visible, one near-infrared, and two mid-infrared) and 120-m ground resolution in one band (thermal infrared) (Lillesand and Kiefer, 1987). Four Landsat TM subscenes of two active Guatemalan volcanoes were acquired. Each subscene was 512 rows by 512 columns (approximately 15 km by 15 km) centered on the volcanic edifice. The data were radiometrically corrected to account for detector gain and offset, and geometrically corrected to a space oblique mercator map projection (CCT-P format). The geometric correction involved nearest-neighbor resampling for the 1986 images and cubic convolution resampling for the 1987 and 1988 images. Cubic convolution resampling tends to minimize the extremes in the data set, resulting in possible errors in the magnitude and location of thermal anomalies. Therefore, nearest-neighbor resampling is preferred because original radiance values are preserved; however, some duplicate "fill" pixels may occur (Glaze *et al.*, 1989a; Oppenheimer *et al.*, 1993).

Image processing of the subscenes was performed with Decision Images software, Release 4.2, on a 386 PC and with ERDAS software, Version 7.4, on a color Sun 3/60 system.

Department of Geological Engineering, Geology and Geophysics, Michigan Technological University, Houghton, MI 49931.

R.J. Andres is presently at the Center for the Management, Utilization, and Protection of Water Resources, Earth Sciences Department, Tennessee Technological University, Box 5062, Cookeville, TN 38505.

Photogrammetric Engineering & Remote Sensing, Vol. 61, No. 6, June 1995, pp. 775–782.

0099-1112/95/6105–775$3.00/0

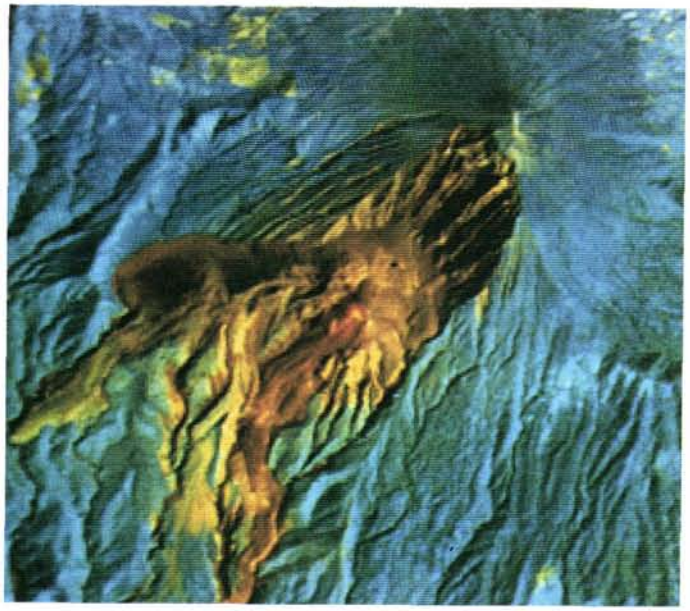

					330 0.0173
	530 0.007	570 0.0128	500 0.02	300 0.08	
	710 0.0024			550 0.0076	510 0.0006
330 0.041	720 0.0022				
	790 0.0007	490 0.0144	740 0.0018		
560 0.0013					North

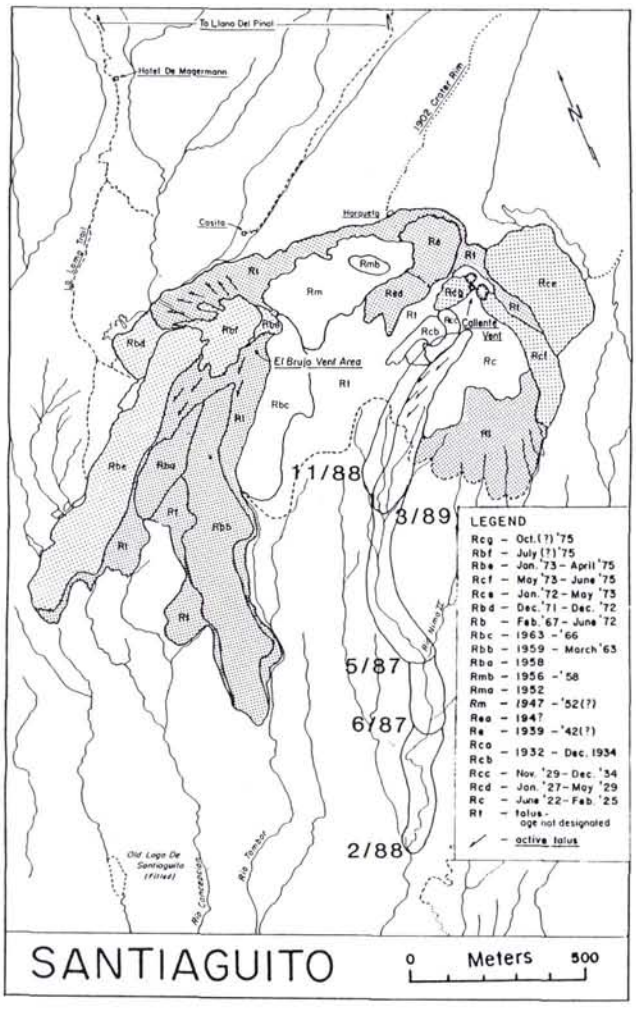

Plate 1. TM subscene, generalized geologic map, and temperature map of the 25 October 1987 Santiaguito Dome thermal anomaly. The thermal anomaly appears as the bright orange area in the center of the image. The 7.3- by 7.1-km subscene displays TM bands 7, 5, and 4 in the red, green, and blue image planes, respectively. This band combination also portrays volcanic rocks in tones of brown, orange, or gray; jungle foliage in blue; and agricultural areas in yellow or green.

The geologic map of the area shows the various exogenous units which comprise the dome, many of which (shaded units) can be clearly seen at the 30-m resolution of the TM subscene. During the two-year period covered by the three TM subscenes, a dacite flow has rapidly advanced down the Rio Nima II watershed. The map shows three successive field-observed flow-fronts. The 1987 subscene allows for another flow front determination, approximately 250 m down slope of the June 1987 field observation. Map modified from SEAN (1988).

Each square on the temperature map represents one pixel of the TM subscene and is approximately 30 m on a side. The upper number in each square represents the thermal anomaly temperature in degrees C. The lower number in each square is the corresponding *f* or fraction of the pixel at that emitting temperature. Lighter squares indicate cooler temperatures, ranging from > 700°C, 400-700°C, to > 300°C. Empty squares do not contain any significant thermal anomaly.

Both software packages were used to take advantage of specific image processing functions unique to each.

Thermal Anomalies

Thermal anomalies in the scenes were located through the thermal infrared band 6 (10.4 to 12.5 μm) which is quantitatively sensitive to temperatures up to 100°C. Above 100°C, the TM sensor for this band saturates and becomes non-quantitative for whole pixel temperature evaluations. Band 6 saturated pixels were then examined for their kinetic temperature, T, by using the radiances recorded in mid-infrared bands 5 (1.55 to 1.75 μm) and 7 (2.08 to 2.35 μm) and the graphical method presented in Rothery *et al.* (1988). This method relies upon the TM sensor radiance calibration constants (Markham and Barker, 1986) and a rearranged version of Planck's radiation law; i.e.,

$$T = c_2 / \lambda \ln([\varepsilon c_1 \lambda^{-5} / \pi R_\lambda] + 1)$$

where c_2 = 0.0144 m K, λ = wavelength (m), ε = emissivity of the radiating surface, $c_1 = 3.742 \times 10^{-16}$ W m^2, R_λ = spectral radiance (W m^{-2} μm^{-1} sr^{-1} (calculated from Equation 1 of Markham and Barker (1986)). An emissivity = 0.8 was used for all calculations and is representative of emissivities used in other studies (Francis and Rothery, 1987; Rothery *et al.*, 1988; Abrams *et al.*, 1991). A ± 0.2 change in emissivity equates to less than a ± 15°C change in temperature. Radiances used in this study were corrected for incident sunlight by subtracting the averaged measured radiance in non-thermally emitting pixels of similar composition and slope aspect in the scene. See Rothery *et al.* (1988) for a more complete description of the method and the inherent errors.

This equation allows for determination of the temperature of subpixel sized thermal features by substituting εf for ε, where f = fraction of the pixel emitting. Under clear sky conditions, reasonable temperatures were obtained for all $f > 0.0005$ or for ground areas greater than 0.4 m^2. Smaller values of f or the presence of clouds gave unrealistically high pixel temperatures. For some pixels, both bands 6 and 7 were saturated. For these pixels, radiances recorded in near-infrared band 4 (0.76 to 0.90 μm) and band 5 were used to determine their temperature; only one of these pixels had $f > 0.0005$ and a reasonable pixel temperature.

Derived temperatures on Santiaguito Dome for a cloud-free TM subscene acquired on 25 October 1987 (scene ID number Y4192715505) are shown in Plate 1. The maximum temperature measured in the thermal anomaly is 790°C and the minimum is 300°C. The anomaly stretches 180 m continuously in the east-west direction. The main region of the anomaly extends 150 m from north to south with one isolated hot pixel lying outside of this continuous region.

This 180- by 150-m thermal anomaly agrees with visual observations of the Caliente vent. The vent consists of 150- by 150-m area covered by rubble through which 600 to 850°C gases pass (Stoiber and Rose, 1969; Stoiber and Rose, 1970; W. Rose, unpublished data). Rock walls of the cracks in zones of high gas emission rates glow red (> 600°C); these zones probably correspond to the pixels with the highest subpixel temperatures. The high gas emission rate zones are surrounded by a region of lower gas emission rates, lower temperatures, and non-glowing rocks; this region is recorded in the TM subscene as pixels with lower subpixel temperatures. The isolated hot pixel lying outside of the continuous thermal anomaly may represent a fumarole field located just outside of the main vent area.

The 14 February 1988 Santiaguito subscene (scene ID number Y4203915550) shows a broad thermal anomaly centered on the dome (Plate 2). It also shows an eruption cloud emanating from the Santiaguito vent. Surrounding the dome is a thin swirl of another cloud, likely erupted a short time prior to the time of the image. The eruption clouds partially obscure the thermal anomaly surrounding the Santiaguito vent and prohibit accurate temperature determinations except for one pixel not obscured by the clouds. This pixel records a temperature of 770°C with an associated f = 0.0034 or 2.8 m^2. It has a temperature similar to that occurring in the corresponding pixel of the 1987 subscene as revealed by image rectification and registration (see next section). The temperatures estimated with other pixels in this image and associated with the thermal anomaly are all unrealistically high ($T \geq 850$°C) and have associated, f's ≤ 0.002. These temperatures, higher than any observed or expected at Santiaguito, likely reflect effects of partial cloud coverage (as explained later), not thermal effects.

The 14 April 1986 Santiaguito subscene (scene ID number Y5077415493) contains a large eruption cloud rising above the dome (Plate 2). This cloud obscures the dome thermal anomaly; thus, no temperatures were determined.

The presence of the eruption cloud in the 1988 and 1986 Santiaguito subscenes causes the measured radiances to increase and thus give anomalously high temperatures for pixels containing such clouds. Calculations using the atmospheric electromagnetic energy propagation model, LOWTRAN7 (Kneizys *et al.*, 1988), show that the presence of the eruption cloud increases multiple scattering in the atmosphere. This scattering increases the amount of energy which is propagated upwards in the atmosphere and, thus, detected by the satellite TM sensor. This gives rise to elevated, calculated radiance levels and, thus, anomalously high temperatures. Cloud-free pixels allow this same energy to travel to the ground surface. Along this path, this energy is absorbed because of the rapidly increasing water vapor concentrations as the ground surface is approached (Gao and Goetz, 1991).

Derived temperatures on Pacaya for a cloud-free TM subscene (scene ID number Y5077415493) acquired on 14 April 1986 are shown in Plate 3. The maximum temperature measured in the thermal anomaly is 820°C and the minimum is 210°C. The discontinuous anomaly stretches 720 m in the east-west direction and 390 m in the north-south direction. One pixel temperature was derived with bands 4 and 5; this resulted in a temperature of 750°C with an associated f = 0.0115. This was necessary because both bands 6 and 7 were saturated and may represent the first time the temperature of a volcanic feature has been determined with these two bands.

The thermal anomaly in the Pacaya subscene is interpreted to be an active, basaltic lava flow. An on site report, one month previous to the satellite acquisition date, indicates that an active lava flow was being issued from the northwest flank of Pacaya (SEAN, 1986). A flow erupted on this flank of the volcano would be channeled to the west and south by the existing topography. This report supports the interpretation of the thermal anomaly as a lava flow in both its origin and subsequent downhill movement.

The discontinuous nature of the Pacaya thermal anomaly is also consistent with the style of lava flows commonly issued from Pacaya. In general, the flow averages a surface temperature of 400 to 500°C with areas of less than 270°C separating the warmer portions of the flow. Also, cooler temperatures occur around the warmest parts of the flow. This thermal fingerprint is characteristic of aa and pahoehoe flows which are flowing downhill over irregular topography. As the underlying topography steepens, the flow velocity increases, and the cooled crust on top of the flow thins and cracks. This allows for more heat to escape from the interior of the flow over areas of steeper slope; thus, the surface temperature of the flow may be higher in some cases then the near-vent temperature. Similar downflow temperature increases have been observed in the 1989 Lonquimay flow, and these also were partially ascribed to changes in topography (Oppenheimer, 1991).

Similar results for the size and temperature of thermally anomalous pixels in these images were obtained using the alternative method presented by Oppenheimer *et al.* (1993). This method assumes the temperature of the high temperature feature and calculates its area and the average temperature of the remaining portion of the pixel. This alternative methodology is used because of the important influence on calculated temperatures of large fractions of cool ground ap-

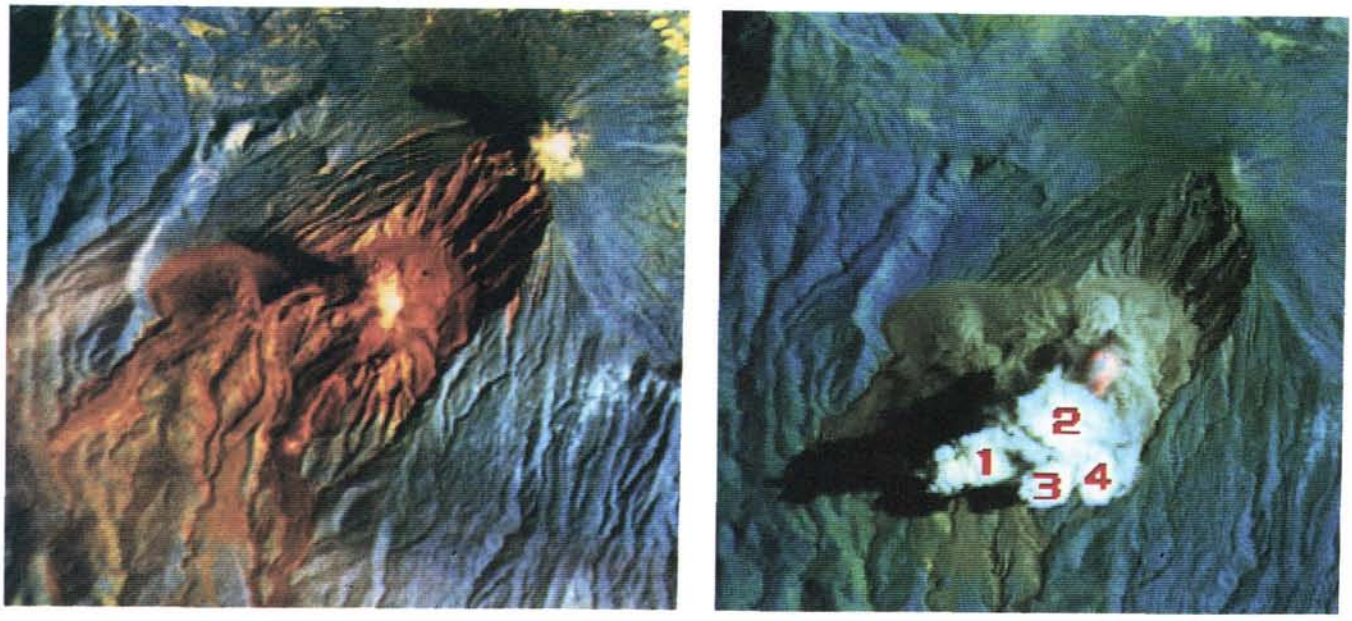

Plate 2. TM subscene of the 14 February 1988 Santiaguito Dome thermal anomaly (left). Display information is the same as in Plate 1. The thermal anomaly is partially obscured by the rising eruption cloud. The associated shadow (yellow to white) appears bifurcated because a higher, more dispersed, sunlit, previously erupted cloud overlies it. The overlying cloud was originally carried west by the winds, but is swirled towards the east when the cloud had risen above a ridge just outside and to the west of the subscene. Another cloud (meteoric) is visible at the summit of Santa María and also casts a long shadow.

TM subscene of the 14 April 1986 Santiaguito Dome thermal anomaly (right). Display information is the same as in Plate 1. The four main lobes of a rising eruption cloud are numbered. To the left is the associated shadow. The orange thermal anomalies occur at the base of the cloud.

pearing in each pixel. The good agreement between the two methods suggests that a sharp border exists between the warmer and cooler regions in each pixel. Field observations support this suggestion as it is common to find thermally unperturbed ground very close, oftentimes within a metre, to a high temperature feature, such as a fumarole field or lava flow.

Temporal Changes of the Santiaguito Thermal Anomaly

Image rectification and registration were used to examine the series of three Santiaguito subscenes to determine if the shape and distribution of the thermal anomalies changed over the two-year period. Rectification is the process of warping the image to a map projection; in this study, two of the Santiaguito subscenes were rectified to the map projection of the third. Registration is the process of overlaying two images so that similar features on each image lie atop each other. Rectification and registration were necessary because, despite being portrayed in the same map projection, each image was displayed with different projection parameters by EOSAT. This occurred because the images were taken from two different satellites which have different orbital characteristics.

After registration, the subscenes were examined for changes in the appearance of thermal anomalies by examining bands 5, 6, and 7 individually. For example, the red image plane contained band 5 of the 1986 subscene, the green image plane contained band 5 of the 1987 subscene, and the blue image plane contained band 5 of the 1988 subscene. The areal extent of the thermal anomalies for each year were then mapped and changes were noted.

Because rectification can change the radiance value recorded in each pixel, rectified subscenes were only used to determine the change in size and shape of thermal anomalies. They were not used to determine temperatures of these anomalies because of the potential problems of working with doubly resampled data (Lillesand and Kiefer, 1987).

Although the eruption cloud did not allow accurate temperature determinations in the 1986 Santiaguito subscene, it did not completely obscure the location of the thermal anomaly on the dome. Unfortunately, only band 7 maps the extent of the thermal anomalies; bands 5 and 6 are obscured by the cloud. Band 7 shows four distinct regions of elevated temperature on the dome in 1986: all are in the Caliente vent region (Figure 1). By 1987, three of these anomalies have disappeared and the remaining anomaly doubled in size. An anomaly also appeared southeast of the main anomaly, but it disappeared by 1988. The other anomaly of 1987 also halved in size by 1988.

This series of subscenes begins to create a baseline by which to judge future thermal anomaly changes. Because volcanic activity at Santiaguito remained relatively constant in both frequency and intensity from 1986 to 1988, we conclude that the areal extent of the Santiaguito thermal anomaly has not changed significantly over this same period. Continued monitoring of the Santiaguito thermal anomaly may forecast significant changes in eruption location, intensity, or style.

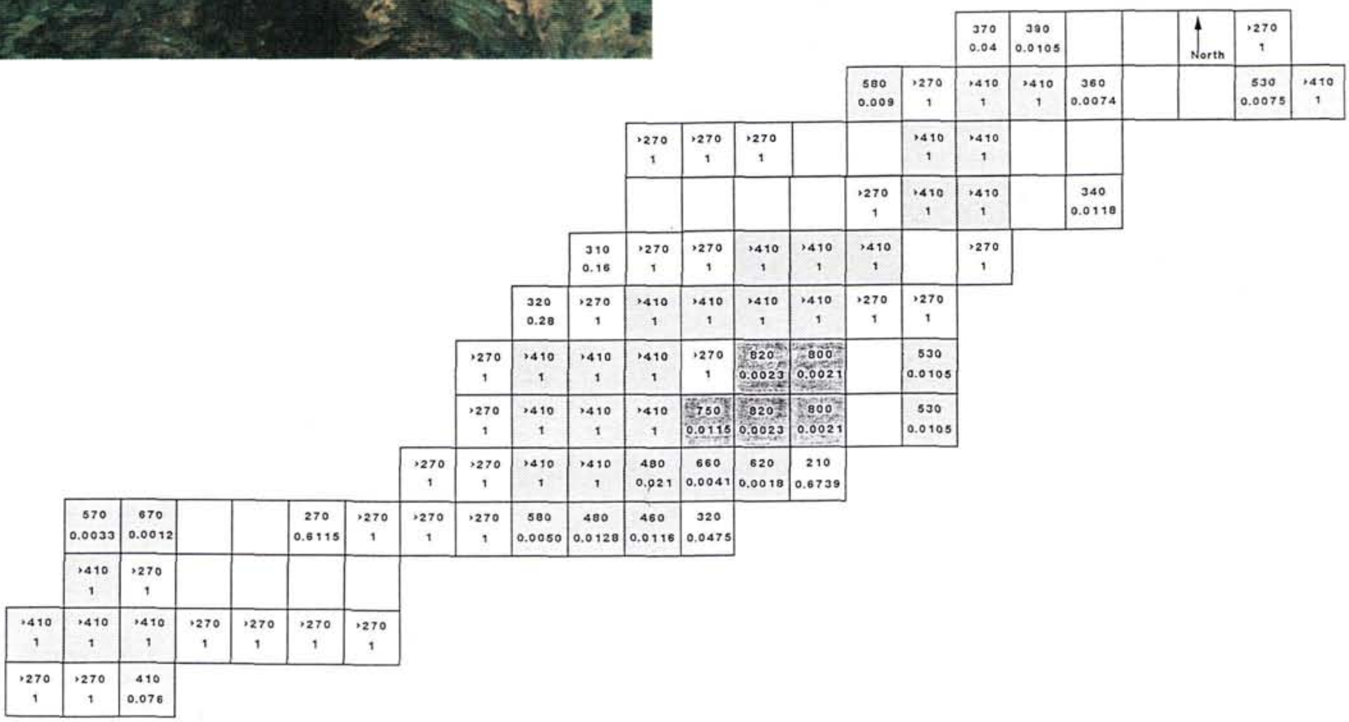

Plate 3. TM *subscene and temperature map of the* 14 April 1986 Pacaya thermal anomaly. The 6.8- by 6.4-km image was created by portraying TM band 5, 2, and 1 in the red, green, and blue image planes, respectively. The thermal anomaly appears as the red linear feature in the image and is interpreted to be an active lava flow traveling from near the Pacaya summit (on the right) downslope (to the left). This band combination also displays unvegetated lava flows in dark tones, forest in blue, and agricultural areas in yellow. Band 7 was not used in this image *reproduction due to its saturation* by the lava flow which manifests itself as streaks in the image.

Each square on the temperature map represents one pixel of the TM subscene and is approximately 30 m on a side. The upper number in each square represents the thermal anomaly temperature in degrees C. The lower number in each square is the corresponding *f* or fraction of the pixel at that emitting temperature. Lighter squares indicate cooler temperatures, ranging from > 700°C, 400-700°C, to > 270°C. Empty squares do not contain any significant thermal anomaly. Pixels with saturated bands are reported as T > 270°C and T > 410°C when bands 7 and 5 are saturated, respectively. These are *the minimum, whole-pixel temperatures* which would saturate these bands, but would not allow more accurate temperature determinations with bands 5 and 4 or 4 and 3, respectively. The paired adjacent pixels which contain 820, 800, and 530°C features may represent duplicate fill pixels.

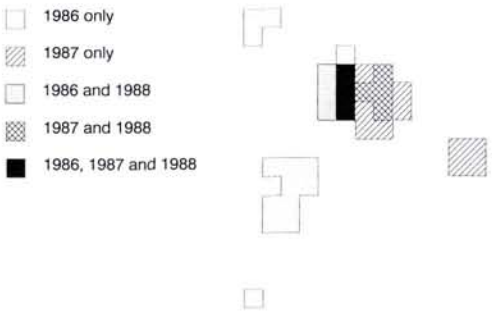

Figure 1. Temporal changes of the Santiaguito thermal anomaly as mapped in TM band 7. The lone square in the map representing the southernmost extent of the 1986 thermal anomaly corresponds to one pixel in the TM image and represents a 30- by 30-m area. North is at the top of the map. Band 7 was used to create the map because it records the location of the thermal anomaly in all three subscenes. The shape and extent of the thermal anomalies shown in the map are approximate; absolute shape and extent are impossible to define at this 30-m resolution.

Image rectification and registration also allowed for examination of the ongoing erosion of the northern face of Santiaguito Dome. Field reports indicate significant erosion of this face began since July 1989 (GVN, 1990; GVN, 1992). Photographs taken from the nearby Santa María summit in January 1988 show that some erosion was in progress by that date (J. Fink, unpublished data). The timing of the beginning of this erosive event is poorly constrained. The satellite images show that no significant erosion occurred between April 1986 and February 1988. Therefore, the erosive event probably began shortly before the January 1988 photos. The erosion is significant because an enormous amount of material is being washed down the local drainages, altering the local fluvial and transportation networks.

Eruption Cloud Heights

Two methods were used to determine eruption cloud heights. Because a Landsat image is essentially a static picture of a dynamic plume which may not have completed its rise, the calculated heights are minimal eruptive heights.

The first method used band 6 radiances to calculate temperatures of the cloud tops and the land surface. This method assumes that the cloud tops are in thermal equilibrium with the surrounding atmosphere. The difference in temperature was then divided by the average atmospheric lapse rate of 6.4°C/km (Cooper and Alley, 1986).

The second method determined plume height by the length of the shadow it cast on the sloping ground and the sun angle (Iqbal, 1983). This method gives a maximum plume height because a vertically rising plume is assumed. A similar shadow method was used by Glaze *et al.* (1989b) to determine plume heights from GOES satellite data. This method can be used to check the thermal equilibrium assumption of the atmospheric lapse rate method. Comparison of absolute plume temperature with radiosonde data was not done in this study because of the distance to the nearest radiosonde release point (approximately 120 km from Santiaguito and in a distinctly different climatic setting).

The large eruption cloud in the 1986 Santiaguito subscene contains four main lobes (Plate 2). Band 6 derived temperatures show that three of these lobes are the same temperature (16°C) and that the fourth lobe is 3 degrees warmer. Assuming the cloud tops are in thermal equilibrium with the surrounding air, the three lobes are at the same altitude. The atmospheric lapse rate gives a rise for these lobes of 4.6 km. The fourth lobe rose 4.1 km. The shadow method for the tip of lobe 1 gave a plume height of 5.0 km. The shadow plume height is an overestimate because the plume has bent towards the west-southwest by the local winds.

The atmospheric lapse rate method calculates a plume height of 1.3 km for the small eruption cloud in the 1988 Santiaguito subscene. The shadow method calculates a maximum plume height of 1.6 km. Although the plume appears to be rising vertically in this subscene, solar azimuth calculations show that it is actually rising at an angle approximately 10° west of north because of the local winds. The thin swirl of clouds also present in the subscene supports this local wind direction. Thus, the height calculated by the shadow method is an overestimate of the true plume height. Table 1 contains a summary of the eruption cloud heights determined by both methods at Santiaguito. Similar eruption cloud heights have been observed at Santiaguito.

In the 1986 Santiaguito subscene, the similar lobe top temperatures and the distance between the lobe tops and their associated shadows suggest that these lobes have undergone similar eruptive dynamics and are all at nearly the same altitude (Table 1). Their identical temperatures suggest that they are all in equilibrium or are all in the same state of disequilibrium with the surrounding atmosphere.

The multi-lobed appearance of the rising plume may have been caused by the irregular geometry of the Caliente vent. A well-defined pit does not exist at Caliente; instead, vertical ash eruptions are emitted from a rubble-filled depression. The rubble disrupts the leading edge of the escaping gases. Multi-lobed eruptive plume tops are commonly observed at Santiaguito.

The fourth lobe is the smallest and was likely erupted after the three lobes discussed above (Table 1). This is supported by its relative upwind location, closer to the vent.

The eruption cloud heights in the 1988 Santiaguito subscene also agree well (Table 1). For both subscenes, the eruption cloud heights calculated by the average atmospheric lapse rate and shadow methods agree to within 0.4 km. The close agreement between the two independent methods suggests that the eruption clouds were in thermal equilibrium with the surrounding air.

TABLE 1. SANTIAGUITO ERUPTION CLOUD HEIGHTS

Year	Lobe	Height (km) as determined by atmospheric lapse rate	Height (km) as determined by shadow method
1986	1-3	4.6	5* (maximum)
	4	4.1	
1988	—	1.3	1.6 (maximum)

* shadow method used on lobe 1 only.

Conclusions

Landsat TM imagery is regularly acquired by satellite and offers a supplementary tool to monitor active volcanoes, especially those not frequently visited. In general, TM data can provide

- a view of the activity of a volcano and its changes since the last on-site visit or imaging date;
- the location, size, shape, and temperature of thermal anomalies (i.e., lava flows, fumarole fields, ...); and
- data on the minimum intensity of eruptions.

Results from examination of the four subscenes from 1986 to 1988 of Santiaguito and Pacaya Volcanoes, Guatemala, include

- the approximate location, size, shape (within the 30-m resolution of the data), and temperature of the thermal anomaly on the Santiaguito dome over a two-year period when in the absence of obscuring clouds;
- Santiaguito eruption cloud heights of up to 5 km;
- better constraint on the beginning of the erosional episode on the north face of Santiaguito; and
- the approximate location, size, shape, and temperature of the active lava flow on Pacaya.

The use of TM data for supplemental monitoring of active volcanoes could be enhanced by development of better algorithms and applications of the data. For example, if the interfering effects of eruption clouds could be modeled and thus removed, then more temperature determinations could be made. This modeling might also allow calculation of water vapor emissions as suggested by Andres (1992). Also, the two-band method presented in Rothery *et al.* (1988) needs more rigorous verification through field studies (Flynn *et al.*, 1989; Oppenheimer and Rothery, 1991; Andres, 1994). This would allow for a better assessment of errors associated with the method.

Added Note

Santa María Volcano has been designated as a Decade Volcano by the International Association of Volcanology and Chemistry of the Earth's Interior as part of the International Decade for Natural Disaster Reduction. Because of this and the success of this preliminary report, a comprehensive study of a variety of remote sensing techniques at this volcano is beginning, with the overall objective of mitigating hazards there.

Acknowledgments

A. MacKenney provided his detailed record of activity at Pacaya to help in the interpretation of that subscene. J. Fink provided photographs of the north face of Santiaguito. L. Glaze and several anonymous reviewers helped improve this manuscript. Volcanic research in Guatemala has been funded by a number of different NSF grants; the most recent was EAR-8916323.

References

Abrams, M., L. Glaze, and M. Sheridan, 1991. Monitoring Colima Volcano, Mexico, using satellite data, *Bull. Volcanol.*, 53:571-574.

Andres, R. J., 1992. *Remote Sensing of Volcanic H_2O, CO_2 and SO_2 Emissions*, Ph.D. Dissertation, Michigan Technological University, Houghton, Michigan, 167 p.

———, 1994. Field test verification of the two satellite band temperature determination method (in preparation).

Andres, R. J., W. I. Rose, R. E. Stoiber, S. N. Williams, O. Matías, and R. Morales, 1992. A summary of sulfur dioxide emission rate measurements from Guatemalan volcanoes, *Bull. Volcanol.* 55:379-388.

Bornhorst, T. J., W. I. Rose, Jr., and L. E. Bornhorst, 1984. Magma evolution in shallow high-Al basalt bodies below Pacaya Volcano, Guatemala, *EOS.*, 65:1153.

Cooper, C. D., and F. C. Alley, 1986. *Air Pollution Control: A Design Approach*, PWS Publishers, Boston, Massachusetts, pp. 507-508.

Eggers, A. A., 1971. *The Geology and Petrology of the Amatitlán Quadrangle*, Guatemala,. Ph.D. Dissertation, Dartmouth College, Hanover, New Hampshire, 221 p.

———, 1983. Temporal gravity and elevation changes at Pacaya Volcano, Guatemala, *J. Volcanol. Geotherm. Res.*, 19:223-237.

Flynn, L. P., P. J. Mouginis-Mark, and J. C. Gradie, 1989. *Radiative Temperature Measurements at Kilauea Volcano, Hawaii*, New Mexico Bureau of Mines and Mineral Resources Bulletin 131, p 94.

Francis, P. W., and D. A. Rothery, 1987. Using the Landsat Thematic Mapper to detect and monitor active volcanoes: An example from Lascar volcano, northern Chile, *Geol.*, 15:614-617.

Gao, B.-C., and A. F. H. Goetz, 1991. Cloud area determination from AVIRIS data using water vapor channels near 1 μm, *J. Geophys. Res.*, 96:2857-2864.

Glaze, L., P. W. Francis, and D. A. Rothery, 1989a. Measuring thermal budgets of active volcanoes by satellite remote sensing, *Nature*, 338:144-146.

Glaze, L. S., P. W. Francis, S. Self, and D. A. Rothery, 1989b. The 16 September 1986 eruption of Lascar volcano, north Chile: Satellite investigations, *Bull. Volcanol.*, 51:149-160.

GVN Bulletin, 1990. Smithsonian Institution, Washington, D. C., 15(3):19-20.

———, 1992. Smithsonian Institution, Washington, D. C., 17(5):9-10.

Iqbal, M., 1983. *An Introduction to Solar Radiation*, Academic Press, Toronto, Canada, pp. 6-27.

Kneizys, F. X., E. P. Shettle, L. W. Abreu, J. H. Chetwynd, G. P. Anderson, W. O. Gallery, J. E. A. Selby, and S. A. Clough, 1988. *Users Guide to LOWTRAN7*, AFGL-TR-88-0177, ERP No. 1010, 146 p.

Lillesand, T. M., and R. W. Kiefer, 1987. *Remote Sensing and Image Interpretation, Second Edition*, John Wiley & Sons, New York, N.Y., pp. 539, 561-569, 612-616.

Markham, B. L., and J. L. Barker, 1986. Landsat MSS and TM post-calibration dynamic ranges, exoatmospheric reflectances and at-satellite temperatures, *EOSAT Tech. Notes*, 1:3-8.

McClelland, L., T. Simkin, M. Summers, E. Nielsen, and T. C. Stein (editors), 1989. *Global Volcanism 1975-1985*, Prentice-Hall, Englewood Cliffs, New Jersey, pp. 475-492.

Mouginis-Mark, P. J., D. Pieri, P. W. Francis, L. Wilson, S. Self, W. I. Rose, and C. A. Wood, 1989. Remote sensing of volcanoes and volcanic terrains, *EOS*, 70:1567-1575.

Mouginis-Mark, P., S. Rowland, P. Francis, T. Friedman, H. Garbeil, J. Gradie, S. Self, L. Wilson, J. Crisp, L. Glaze, K. Jones, A. Kahle, D. Pieri, H. Zebker, A. Krueger, L. Walter, C. Wood, W. Rose, J. Adams, and R. Wolff, 1991. Analysis of active volcanoes from the Earth Observing System, *Rem. Sens. Environment*, 36: 1-12.

Mouginis-Mark, P. J., and P. W. Francis, 1992. Satellite observations of active volcanoes: Prospects for the 1990s, *Episodes*, 15:46-55.

Oppenheimer, C., 1991. Lava flow cooling estimated from Landsat Thematic Mapper infrared data: The Lonquimay eruption, *J. Geophys. Res.*, 96:21865-21878.

Oppenheimer, C., P. W. Francis, D. A. Rothery, R. W. T. Carlton, and L. S. Glaze, 1993. Infrared image analysis of volcanic thermal features: Lascar Volcano, Chile, 1984-1992. *J. Geophys. Res.*, 98: 4269-4286.

Oppenheimer, C. M. M., and D. A. Rothery, 1991. Infrared monitoring of volcanoes by satellite. *J. Geol. Soc. Lond.*, 148:563-569.

Rose, Jr., W. I., 1972. Santiaguito Volcanic Dome, Guatemala. *Geol. Soc. Am. Bull.*, 83:1413-1434.

Rothery, D. A., P. W. Francis, and C. A. Wood, 1988. Volcano monitoring using short wavelength infrared data from satellites. *J. Geophys. Res.*, 93:7993-8008.

SEAN Bulletin, 1986. Smithsonian Institution, Washington, D. C., 11(3):12-13.

———, 1988. Smithsonian Institution, Washington, D. C., 13(11):2-5.

Stoiber, R. E., and W. I. Rose, Jr., 1969. Recent volcanic and fumarolic activity at Santiaguito Volcano, Guatemala, *Bull. Volcanol.*, 2:475-502.

———, 1970. The geochemistry of Central American volcanic gas condensates, *Geol. Soc. Am. Bull.*, 81:2891-2912.

Wunderman, R. L., and W. I. Rose, 1984. Amatitlan, an actively resurging cauldron 10 km south of Guatemala City, *J. Geophys. Res.*, 89:8525-8539.

(Received 11 August 1992; revised and accepted 1 June 1993; revised 12 August 1993)

Robert J. Andres
Robert J. Andres is a postdoctoral researcher at Tennessee Technological University and Oak Ridge National Laboratory. He has conducted research on active volcanoes for seven years, specializing in the geochemistry of their emissions and developing new remote methods for their detection and measurement. He has also been involved with validation of existing remote measurement techniques.

William I. Rose
William I. Rose is professor and Department Head of the Department of Geological Engineering, Geology and Geophysics at Michigan Tech. He has been doing research at active volcanoes for more than 25 years, and has been particularly interested in studying volcano/atmosphere interactions. Satellite remote sensing of volcanic clouds and plumes has been his main research focus in recent years. He leads a new Laboratory of Atmospheric Remote Sensing, an interdisciplinary facility at Michigan Tech.